Supporting Information

SI Materials and Methods

Plant Materials and Growth Conditions. Seeds of wild type rice cultivar Nipponbare (*Oryza sativa* L. cv. Nipponbare) were obtained from Prof. Xiao-Ya Chen (Shanghai Institutes for Biological Sciences, Chinese Academy of Sciences). Seeds of wild type rice cultivar Donjing (*O. sativa* L. cv. Donjing) and T-DNA insertion lines *osggpps-1* (1B-10639) and *osgrp-1* (2C-60311) were obtained from Kyung Hee University (Korea). Wild type and transgenic rice plants were grown in the greenhouse and growth chamber under 14-h-light/10-h-dark cycles at 28/20°C day/night temperature and 70% relative humidity. The light intensity was controlled at 150 μmol $m^{-2}s^{-1}$.

RNA Extraction, cDNA Synthesis, and qRT-PCR. Samples used for RNA extraction were frozen in liquid nitrogen and stored at -80°C until use. Total RNA was extracted using the RNAiso reagent (TaKaRa, Shiga, Japan) and treated with DNaseI (Promega, Madison, WI) to eliminate genomic DNA contamination. 1 μg of total RNA from each sample was used for first-strand cDNA synthesis by using PrimeScript 1st strand cDNA synthesis kit (TaKaRa) following the manufacturer's protocol. The quantitative real-time PCR (qRT-PCR) was performed using SYBR Premix ExTaq II (TaKaRa) in a Thermal Cycler Dice Real Time System TP800 (TaKaRa), according to the manufacturer's instructions. Primer sequences are listed in Table S4. After an initial denaturation step at 95°C for 30 s, the template was amplified for 40 cycles of denaturation for 5 s at 95°C, annealing of primers for 15 s at 55°C, and extension for 20 s at 72°C. Fluorescent data were acquired during each extension phase. After amplification, a melting curve was generated ranging from 95°C to 60°C to check for product specificity. Gene expression values were calculated according to the comparative C_T method (1). *OsActin* (*Os03g50885*) was used as a reference. Each data point represents at least three independent biological samples, with three or more technical replicates.

Phylogenetic Analysis. Sequences of rice PTS homologs were obtained by BLAST search against the rice genome database (http://rice.plantbiology.msu.edu/) using PTSs from *Arabidopsis thaliana*. The full-length amino acid sequences were aligned by using

ClustalW (2) and the neighbor-joining phylogenetic tree was constructed by using MEGA6 (3) with default settings. The scale bar corresponds to 20% amino acid sequence divergence.

Generation of Binary Vectors and Plant Transformation. For overexpression, coding regions of *OsGGPPS1* and *OsGRP* were cloned into the pRTL2 vector carrying the *CaMV 35S* promoter (4). The entire expression cassette was then excised and subcloned into pCAMBIA1300 (CAMBIA, Canberra, Australia). To generate RNAi transgenic plants, specific fragments of *OsGGPPS1* and *OsGRP* cDNA sequences were amplified and cloned in sense and antisense orientations into the pFGC5941 vector (ABRC, Ohio State University, Columbus, OH). Primers are detailed in Table S4. The resulting plasmids were transformed into *Agrobacterium tumefaciens* strain EHA105. Callus of the rice Nipponbare cultivar was transformed as described previously (5), pCAMBIA1300 was used as an empty vector control. T1 seedlings were grown on Murashige and Skoog (MS) medium containing 3g/L phytagel (Sigma-Aldrich, St. Louise, MO) and 50 mg/L hygromycin (for pCAMBIA1300) or 30 mg/L Basta (for pFGC5941) for selection. Untransformed rice plants were used as a control. Selected rice plants were grown in paddy field during the natural growing season for seed propagation. T2 plants were grown in greenhouse or growth chamber for phenotype observations and further analyses.

Bacterial Pigment Complementation Assay. The construct pAC-94N was a gift from Dr. Francis X. Cunningham Jr. (University of Maryland) (6). Four candidate plastidic *PTS* genes with their fragments corresponding to putative transit peptides truncated (the truncation sites are shown in Fig. S1) were cloned into pET32b (Novagen, Madison, WI). OsGRP was also subcloned into pET28a (Novagen) for co-expression with pET32b-OsGGPPS1. To determine GGPPS activity, the resulting constructs were co-transformed with pAC-94N into *E. coli* BL21(DE3) cells (Novagen). Positive co-transformed colonies were used to inoculate 8 mL Luria-Bertani (LB) medium containing 34 μg/mL chloramphenicol and 100 μg/mL ampicillin (for the co-expression of both pET32b-OsGGPPS1 and pET28a-OsGRP with pAC-94N, 50 μg/mL kanamycin was also added). One mL of the overnight culture was transferred to 100 mL of the same medium and continued to grow at 37°C to reach an OD_{600} of 0.3. Protein expression was induced by

adding isopropyl β-thiogalactopyranoside (IPTG) to a final concentration of 1mM. After growing for 16 h at 18°C, bacterial cells were harvested by centrifugation and equal wet weights of pelleted cells from different transformants were re-suspended in 200 μL water in 96 well plates for photographing. For carotenoid quantification, the same wet weight pellet was re-suspended in 80% (v/v) acetone to extract the pigments and the absorbance at 440 nm was measured. Functionally characterized *GGPPS* from *Antirrhinum majus* (*AmLSU*) (7) and the pET32b empty vector were used as positive and negative controls, respectively.

Expression and Purification of Recombinant Proteins. For enzymatic assays, *OsGPPS* and *OsGGPPS1* without their fragments corresponding to putative transit peptides were cloned upstream and in-frame of the $(His)_6$-tag sequences in pET32b to express OsGPPS-His and OsGGPPS1-His recombinant proteins. *OsGRP* without the region for putative transit peptide was cloned into pET28a downstream and in-frame of the $(His)_6$-tag sequence to express His-OsGRP recombinant proteins. For co-expression with His-OsGRP, truncated *OsGGPPS1* with a stop codon was cloned into pET32b to express non-tagged OsGGPPS1. Restriction sites and primers used are detailed in Table S4. The resulting recombinant plasmids were transformed into *E. coli* Rosetta2(DE3)pLysS cells (Novagen) individually or co-transformed with two plasmids in a single transformation event. Single positive colonies were used for growth and induction as described above. Induced cells were harvested by centrifugation and stored at -80°C until use. The recombinant His-tagged proteins were purified using nickel-nitrilotriacetic acid (Ni-NTA) agarose (Qiagen, Hilden, Germany) according to the manufacturer's instruction. Protein concentration was determined according to Bradford (8).

Site-Directed Mutagenesis. Site-directed mutations of OsGRP were introduced using overlap extension PCR as described previously (9). Primers for mutagenesis are detailed in Table S4. The mutated *OsGRP*s were sub-cloned into pET28a for the expression of the His-tagged OsGRP mutant proteins. The resulting constructs were confirmed by DNA sequencing.

Enzymatic Assay and Product Identification. For determination of the *in vitro* activity of rice PTS homologs using LC-MS/MS, the enzymatic activity assays were performed in a final volume of 200 µL containing 40 µM IPP and 40 µM co-substrate (DMAPP, GPP or FPP) in assay buffer (25 mM MOPSO, pH 7.0, 10% [v/v] glycerol, 2 mM DTT, and 10 mM $MgCl_2$) and 1 µg of purified recombinant proteins. The assay mixture was incubated for 1h at 30°C, stopped by freezing in liquid N_2. Proteins were denatured as described before (10, 11) by adding 500 µL of chloroform and vortexing. After centrifugation at 3000 *g* for 5 min, the water phase was transferred to a glass vial for LC-MS/MS analysis. The analyses of isoprenoid products were performed on a Waters Quattro Premier XE LC/MS/MS (Waters, Milford, MA), data were collected and analyzed using Masslynx v4.1 software (Waters). Separation was performed using an Acquity BEH C18 UPLC column (1.7 µm, 2.1 × 50 mm; Waters). The injection volume was 10 µL. A solvent system containing solution A (0.05% triethylamine in water, pH 5-6) and solution B (50:50 acetonitrile/isopropanol) was used with the following gradient: 0-0.5 min isocratic with 95% A, 0.5-3.0 min linear from 95% A to 1% A, 3.0-4.0 min isocratic with 1% A, 4.0-5 min linear from 1% A to 95% A. The flow rate was 0.3 mL/min and the column temperature was 50°C. The mass spectrometer was used in negative electrospray ionization mode with the following parameters: capillary voltage 2.5 kV, cone voltage 35 V, source temperature 120°C, desolvation temperature 350°C, cone gas flow 50 L/h, desolvation gas flow 800 L/h. The calibration curves for commercial GPP, FPP and GGPP were prepared as external standards. Two injections were performed at various concentrations (0.1 to 200 pmol), and the standard curves were constructed by plotting the peak area versus concentration and fitting a line.

Kinetic Analysis. For kinetic studies, appropriate concentrations of purified recombinant proteins were used so that the reaction velocity was propotional to the enzyme concentration and was linear with respect to incubation time. The enzyme assays were performed using [1-^{14}C]-IPP as described previously (12). Radiolabeled [1-^{14}C]-IPP (55 mCi/mmol) was purchased from American Radiolabeled Chemicals (St. Louis, MO). The reactions were performed in a final volume of 100 µL containing appropriate concentrations of [1-^{14}C]-IPP and co-substrate (DMAPP, GPP or FPP) in assay buffer (25

mM MOPSO, pH 7.0, 10% [v/v] glycerol, 2 mM DTT, and 10 mM $MgCl_2$). After initiation of reaction by addition of the protein, it was overlaid with 1 mL of hexane and incubated for 10 min at 30°C. To stop the reaction and hydrolyze the products, 10 μL of 3N HCl was added to the samples and then incubated for 20 min at 30°C. The hydrolysis products were extracted into the hexane phase by vigorous mixing for 15s. 800 μL of the hexane phase was used for total radioactivity determination by liquid scintillation counter (LS 6500, Beckman Coulter, Indianapolis, IN). In addition, kinetic parameters were determined by LC/MS-MS, which resuled in similar values (Table S2). The concentrations of DMAPP, GPP, FPP and IPP were varied, whereas the corresponding co-substrates were kept at saturating concentrations. Assays containing boiled protein extracts were used as controls. The background radioactivity produced in the controls was subtracted from all results. A nonlinear regression analysis in GraphPad Prism 6.0 (GraphPad, La Jolla, CA) was used to calculate the kinetic parameters.

Protein Extraction and Immunoblot Analysis. Chloroplast isolation and sub-fractionation were carried out as described previously using freshly harvested leaves of 4-week-old Nipponbare cultivar plants (13, 14). For immunoblot analysis, identical amounts of protein sample were mixed with an equal volume of 2 × SDS loading buffer (15), denatured and separated by 12% SDS-PAGE and blotted onto nitrocellulose membranes by the semi-dry transfer method.

Based on the amino acid sequences of OsGGPPS1, OsGRP, OsGGR, OsLIL3, OsPORB and OsCHLG, specific peptides were designed (Table S5) and used as antigens to immunize rabbits (GenScript, Nanjing, China). Antibodies against RbcL and Tic110 were purchase from Agrisera (Vännäs, Sweden). Horseradish peroxidase (HRP)-conjugated secondary antibodies against rabbit IgG were purchased from Promega. Immobilon Western HRP substrate for chemiluminescent detection was from EMD Millipore (Darmstadt, Germany).

Blue-Native PAGE Analysis. Isolation of thylakoid membranes were carried out as described previously (16) with minor modifications. Leaves of four-week-old rice Nipponbare cultivar plants were homogenized with ice-cold grinding buffer containing 50

mM HEPES-KOH, pH 7.5, 330 mM sorbitol, 2 mM EDTA, 1 mM $MgCl_2$, 5 mM ascorbate, 0.05% bovine serum albumin, 10 mM NaF, and 1% protease inhibitor cocktail (Sigma-Aldrich). The suspension was filtered through two layers of Miracloth and centrifuged at 2,500 g at 4°C for 4 min. The green pellet was resuspended in shock buffer containing 50 mM HEPES-KOH, pH 7.5, 5 mM sorbitol, 5 mM $MgCl_2$, 10 mM NaF, and 1% protease inhibitor cocktail. After centrifugation for 4 min at 2,500 g at 4°C, the green pellet was washed twice with storage buffer containing 50 mM HEPES-KOH, pH 7.5, 100 mM sorbitol, 10 mM $MgCl_2$, 10 mM NaF, and 1% protease inhibitor cocktail. The pellet containing the membrane proteins was resuspended in storage buffer to a chlorophyll concentration of 1 mg/mL and stored at -80°C until use.

Solubilization of membrane complexes was performed by addition of 1% (w/v) *n*-dodecyl-β-D-maltoside (β-DM, Sigma-Aldrich) and incubation on ice for 10 min. One-dimensional (1D) BN-PAGE was performed using 5-14% acrylamide gradient gels according to the method described before (17). For each lane, protein sample containing 20 μg of chlorophyll was loaded. The separation pattern and molecular sizes of major thylakoid membrane complexes were estimated as described before (18). After electrophoresis, gel strips were blotted and then probed with antibodies raised against OsGGPPS1, OsGRP, OsGGR, OsLIL3, OsPORB and OsCHLG, respectively, as mentioned above.

Duplicate gel strips from 1D BN-PAGE were also incubated with 1% SDS and 1% β-mercaptoethanol for 2 h, and then separated by 12% SDS-PAGE as the 2nd dimension as reported (17). After electrophoresis, proteins were blotted and probed with corresponding antibodies.

Crystallization, Data Collection and Structure Determination. For crystallization, purified proteins were concentrated to around 10 mg/mL before further purification by gel filtration (Superdex-200, GE Healthcare, Pittsburgh, PA). The peak fraction was collected and concentrated to approximately 8 mg/mL. Crystallization was performed by using the sitting drop vapor diffusion method. The OsGGPPS1/OsGGPPS1 crystals were grown under 2.0 M sodium malonate, 20% PEG 3350, pH 7.0, at 20°C. Diffractions of the OsGGPPS1/OsGGPPS1 crystals were collected at 2 Å. Crystals of OsGGPPS1/OsGRP

complex were grown under 16% PEG 10000, 0.1 M Bis-Tris, pH 6.5, at 20°C, and solved at 3.6 Å. All data sets were collected at the BL17U beamline of the Shanghai Synchrotron Radiation Facility (SSRF) and processed with HKL2000 (19). For phase determination of OsGGPPS1, molecular replacement was adopted using the structure geometry of geranylfarnesyl diphosphate synthase 2 from *Arabidopsis thaliana* (PDB ID, 5E8H) (20). OsGGPPS1 was then solved as R_{free}/R_{work}= 0.187/0.213. The chain A of OsGGPPS1 was then set as the starting model for further structure determination for OsGGPPS1/ OsGRP complex. PHENIX (21) were used for phase and refinement, and additional manual refinement were operated in COOT (22).

Rice Protoplast Isolation and Transient Expression. Mature seeds of the Nipponbare rice cultivar were dehulled and treated with 70% ethanol for 1 min. These seeds were further sterilized with 2% sodium hypochlorite for 15 min, washed with sterile water for five times and incubated on half strength MS medium containing 3g/L phytagel. Seedlings were grown under a photoperiod of 14 h light (100 μmol $m^{-2}s^{-1}$) and 10 h dark at 26°C for one week. Rice mesophyll protoplasts were isolated and transfected according to the procedure as described (23, 24) with some alterations. Briefly, green tissues of rice seedlings were cut into approximately 0.5 mm strips with a sharp razor blade. The strips were immediately transferred into the freshly prepared enzyme solution (1.5% cellulase R10, 0.75% macerozyme R10, 0.6 M mannitol, 10 mM MES at pH 5.7, 10 mM $CaCl_2$, 20 mM KCl, 5 mM β-mercaptoethanol and 0.1% BSA) and vacuum infiltrated for 5 min in the dark. The enzyme digestion was continued for 6 h in the dark with gentle shaking. After digestion, an equal volume of W5 solution (2 mM MES at pH 5.7, 154 mM NaCl, 125 mM $CaCl_2$ and 5 mM KCl) was added. Protoplasts were released by filtering through 100 μm nylon meshes into 50 mL centrifuge tubes. Pellets were collected by centrifugation at 100 g for 2 min with a swinging bucket rotor. The protoplasts were resuspended in W5 solution and recovered on ice for 30 min. W5 solution was removed by centrifugation at 100 g for 1 min, the pellets were resuspended in MMG solution (4 mM MES at pH 5.7, 0.4 M mannitol and 15 mM $MgCl_2$) at a concentration of 2×10^6 protoplasts/mL counted by using a hematocytometer.

For PEG-mediated transfection, 10 μL plasmid DNA (1 μg/μL) were mixed with 100

μL protoplasts (about 2×10^5 protoplasts). 110 μL freshly prepared PEG solution (40% PEG4000, 0.2 M mannitol and 0.1 M $CaCl_2$) were added and mixed by gently tapping. The transfection mixture was incubated at room temperature for 15 min in the dark. 440 μL W5 solution was added after incubation and the mixture was mixed well by gently tapping. Protoplasts were pelleted by centrifugation at 100 g for 2 min and resuspended with 250 μL WI solution (4 mM MES at pH 5.7, 0.5 mM mannitol and 20 mM KCl). Finally, the protoplasts were cultured in 24-well plates at room temperature for 16 h in the dark.

Subcellular Localization. pA7-YFP and pSAT4A-mCherry-N1 vectors were obtained from ABRC. cDNAs encoding proteins of interest, including rice PTS homologs and organellar markers, were cloned into these vectors for expression of respective fluorescent reporter constructs in rice protoplasts (Table S4). Full length rice Tic40 (Os04g35900), transit peptide of *Arabidopsis* Rubisco small subunit (RbcS, At1g67090), transit peptide of rice mitochondrial ribosomal protein L6 gene 1 (OsRpl6-1, Os03g51510) (24), signal peptide of *Arabidopsis* wall-associated kinase 2 (WAK2, At1g21270) (24) and full length rice peroxisomal membrane 22 kDa family protein (PMP22, Os02g13270) (25) were fused to the N-terminus of EYFP and used as markers for the localization in envelope and stroma of chloroplasts, mitochondria, endoplasmic reticulum and peroxisomes, respectively. The corresponding constructs were transformed into rice (Nipponbare cultivar) protoplasts by PEG-mediated transfection as described above. Fluorescence signals were observed using a confocal laser scanning microscope (FluoView FV1000, Olympus, Tokyo, Japan). The excitation wavelengths were 515 nm for EYFP and 561 nm for mCherry. The emission filters were 530-560 nm for EYFP and 580-620 nm for mCherry. Chlorophyll autofluorescence was monitored using 635 nm excitation wavelengths, and 650-750 nm detection windows. All transient expression experiments were repeated independently at least three times.

BiFC Assay. The pSAT vectors (26) were obtained from ABRC. The full open reading frames (ORFs) of genes of interest without stop codons were cloned into pSAT1A-cEYFP-N1 and pSAT4A-nEYFP-N1 (detailed in Table S4). The resulting constructs were used for transient expression in rice protoplasts. Ten micrograms of each plasmid was used for PEG-

mediated transformation of 200 μL of the ice-cold protoplasts. Transient expression of the EYFP fusion proteins was observed 16 h after transformation. All figures show representative images from at least five independent experiments.

Yeast Two-Hybrid Assay. The Matchmaker GAL4 two-hybrid system (Clontech, Mountain View, CA) was used. To determine the interactions among PTS proteins, the full length ORF of *OsGGPPS1* was amplified and fused downstream of the DNA binding domain (BD) of pGBK-T7 and the DNA activation domain (AD) of pGAD-T7. The full length ORFs of *OsGRP* and *AtSSU* were fused downstream of the BD of pGBK-T7. The full length ORF of *AtGGPPS11* was fused downstream of the AD of pGAD-T7. Interactions between tested proteins and empty vectors (EV) were used as negative controls, and interactions between AtGGPPS11 and AtSSU were used as a positive control. To determine interactions between OsGGPPS1 and other potential partners, *OsGGPPS1* was fused with BD, while full length ORFs of all other genes were fused with the AD of pGAD-T7. Each pair of constructs to be tested were co-transformed into yeast strain AH109 and spotted on nonselective (-LW) plates for 3 d at 30°C. Transformants were tested for protein-protein interactions by growing on selective (-LWAH) plates containing 40 mg/L X-α-Gal. β-galactosidase activity assays were performed by a liquid assay using *o*-nitrophenyl-β-D-galactopyranoside (ONPG) according to the manufacturer's manual. Primers used to generate the different yeast constructs are listed in Table S4.

Pigment Extraction and Analysis. One hundred milligrams of rice leaf tissues were frozen in liquid nitrogen, ground into fine powder and then extracted with 1 mL 80% acetone. Profiles and concentrations of chlorophylls and carotenoids in the extracts were analyzed by reverse phase HPLC as described previously (27). For each line, three independent biological replicates were quantified (each with three technical replicates).

Statistical Analysis. To determine statistical significance, we employed Student's *t* test. Differences were considered significant at $P < 0.05$.

Accession Numbers. The GenBank accession numbers of the proteins used in the

phylogenetic analysis (Fig. S3) are as follows: AgGPPS1, AF513111; AgGPPS2, AF513112; AgGPPS3, AF513113; PaGPPS, EU432047; PaGPPS/GGPPS, GQ369788; PaGPPS3, EU432048; MiGPPS1, JN035297; MiGPPS2, JN035298; MiFPPS, JN035296; AmGPPS.LSU, AAS82860; AmGPPS.SSU, AAS82859; CbGPPS.SSU, AY534745; CrGGPPS, JX417183; CrGPPS.SSU, JX417184; HlGPPS.LSU, FJ455407; HlGPPS.SSU, ACQ90681; MpGPPS.LSU, AF182828; MpGPPS.SSU, AF182827; VvGPPS, AAR08151; LaFPPS, U15777; AaFPPS, U36376; ZmFPPS, L39789; NtGGPPS1, GQ911583; NtGGPPS2, GQ911584; SlGGPPS1, DQ267902; SlGGPPS2, DQ267903; SaGGPPS, CAA67330; SlSPPS, DQ889204; HbSPPS, DQ437520. AGI numbers for *A. thaliana* PTSs are as follows: AtPPPS, At2g434630; AtFPPS1, At5g47770; AtFPPS2, At4g17190; AtSPPS1, At1g78510; AtSPPS2, At1g17050; AtGGPPS11, At4g36810; AtGGPPS2, At2g18620; AtGPPS.SSUII, At4g38460. Rice PTS homologs are listed in Table S1.

References

1. Schmittgen TD & Livak KJ (2008) Analyzing real-time PCR data by the comparative C_T method. *Nat Protoc* 3(6):1101-1108.
2. Thompson JD, Higgins DG, & Gibson TJ (1994) CLUSTAL W: improving the sensitivity of progressive multiple sequence alignment through sequence weighting, position-specific gap penalties and weight matrix choice. *Nucleic Acids Res* 22(22):4673-4680.
3. Tamura K, Stecher G, Peterson D, Filipski A, & Kumar S (2013) MEGA6: Molecular evolutionary genetics analysis version 6.0. *Mol Biol Evol* 30(12):2725-2729.
4. Lu S, et al. (2006) The cauliflower *Or* gene encodes a DnaJ cysteine-rich domain-containing protein that mediates high levels of β-carotene accumulation. *Plant Cell* 18(12):3594-3605.
5. Hiei Y, Ohta S, Komari T, & Kumashiro T (1994) Efficient transformation of rice (*Oryza sativa* L.) mediated by *Agrobacterium* and sequence analysis of the boundaries of the T-DNA. *Plant J* 6(2):271-282.
6. Cunningham FX, Jr. & Gantt E (2007) A portfolio of plasmids for identification and analysis of carotenoid pathway enzymes: *Adonis aestivalis* as a case study. *Photosynth Res* 92(2):245-259.
7. Tholl D, et al. (2004) Formation of monoterpenes in *Antirrhinum majus* and *Clarkia breweri* flowers involves heterodimeric geranyl diphosphate synthases. *Plant Cell* 16(4):977-992.
8. Bradford MM (1976) A rapid and sensitive method for the quantitation of microgram quantities of protein utilizing the principle of protein-dye binding. *Anal Biochem* 72:248-254.
9. Ho SN, Hunt HD, Horton RM, Pullen JK, & Pease LR (1989) Site-directed mutagenesis by overlap extension using the polymerase chain reaction. *Gene* 77(1):51-59.
10. Nagel R, Gershenzon J, & Schmidt A (2012) Nonradioactive assay for detecting isoprenyl diphosphate synthase activity in crude plants extracts using liquid chromatography couples with tandem mass spectrometry. *Anal Biochem* 422:33-38.
11. Nagel R, et al. (2015) *Arabidopsis thaliana* isoprenyl diphosphate synthases produce the C_{25} intermediate geranylfarnesyl diphosphate. *Plant J* 84:847-859.
12. Orlova I, et al. (2009) The small subunit of snapdragon geranyl diphosphate synthase modifies the chain length specificity of tobacco geranylgeranyl diphosphate synthase in planta. *Plant Cell* 21(12):4002-4017.
13. Hall M, Mishra Y, & Schröder WP (2011) Preparation of stroma, thylakoid membrane, and lumen fractions from *Arabidopsis thaliana* chloroplasts for proteomic analysis. *Methods in Molecular Biology, vol. 775,* Chloroplast Research in Arabidopsis: Methods and Protocols, ed Jarvis RP (Springer, New York), Vol II,

pp 207-222.
14. Salvi D, et al. (2011) Preparation of envelope membrane fractions from Arabidopsis chloroplasts for proteomic analysis and other studies. *Methods in Molecular Biology, vol. 775,* Chloroplast Research in Arabidopsis: Methods and Protocols, ed Jarvis RP (Springer, New York), Vol II, pp 189-206.
15. Sambrook J, Fritsch EE, & Maniatis T (1989) *Molecular Cloning: A Laboratory Manual* (Cold Spring Harbor Laboratory Press, New York), 2nd Ed.
16. Sirpiö S, Suorsa M, & Aro EM (2011) Analysis of thylakoid protein complexes by two-dimensional electrophoretic systems. *Methods in Molecular Biology, vol. 775,* Chloroplast Research in Arabidopsis: Methods and Protocols, ed Jarvis RP (Springer, New York), Vol II, pp 19-30.
17. Wittig I, Braun H-P, & Schägger H (2006) Blue native PAGE. *Nat Protoc* 1(1):418-428.
18. Shao J, Zhang Y, Yu J, Guo L, & Ding Y (2011) Isolation of thylakoid membrane complexes from rice by a new double-strips BN/SDS-PAGE and bioinformatics prediction of stromal ridge subunits interaction. *PLoS One* 6(5):e20342.
19. Otwinowski Z & Minor W (1997) Processing of X-ray diffraction data collected in oscillation mode. *Methods Enzymol* 276:307-326.
20. Wang C, et al. (2016) Structural analyses of short-chain prenyltransferases identify an evolutionarily conserved GFPPS clade in Brassicaceae plants. *Mol Plant* 9(2):195-204.
21. Adams PD, et al. (2010) PHENIX: a comprehensive Python-based system for macromolecular structure solution. *Acta Crystallogr D Biol Crystallogr* 66(Pt 2):213-221.
22. Emsley P, Lohkamp B, Scott WG, & Cowtan K (2010) Features and development of Coot. *Acta Crystallogr D Biol Crystallogr* 66(Pt 4):486-501.
23. Yoo SD, Cho YH, & Sheen J (2007) *Arabidopsis* mesophyll protoplasts: a versatile cell system for transient gene expression analysis. *Nat Protoc* 2(7):1565-1572.
24. Zhang Y, et al. (2011) A highly efficient rice green tissue protoplast system for transient gene expression and studying light/chloroplast-related processes. *Plant Methods* 7(1):30.
25. Kaur N & Hu J (2011) Defining the plant peroxisomal proteome: from *Arabidopsis* to rice. *Front Plant Sci* 2:103.
26. Citovsky V, et al. (2006) Subcellular localization of interacting proteins by bimolecular fluorescence complementation *in planta*. *J Mol Biol* 362(5):1120-1131.
27. Wang YW, et al. (2016) The DnaJ-like zinc finger domain protein PSA2 affects light acclimation and chloroplast development in *Arabidopsis thaliana*. *Front Plant Sci* 7:360.

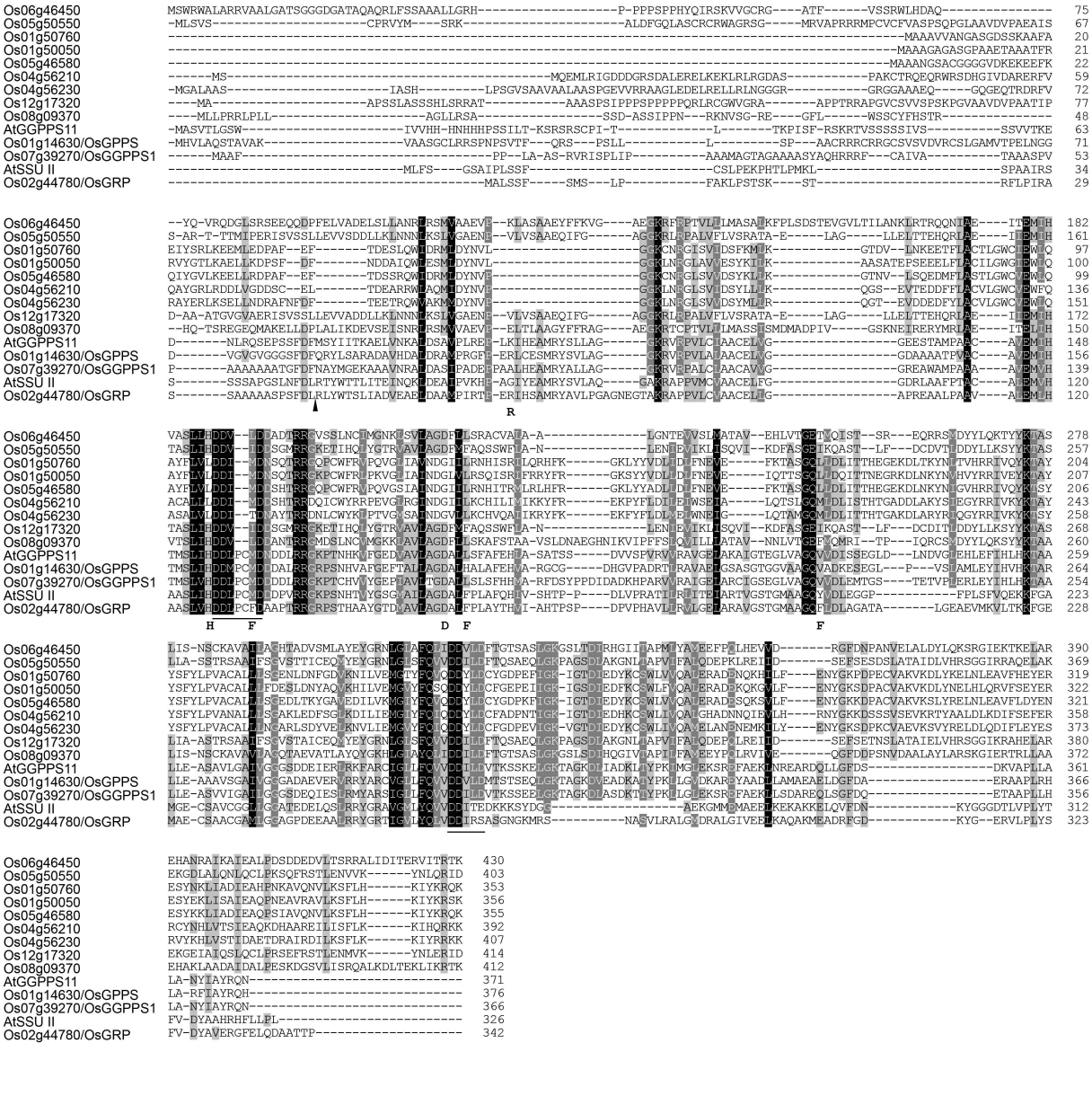

Fig. S1. Sequence analysis of PTS homologs from rice and *Arabidopsis thaliana*. The aspartate-rich motifs are underlined. The six amino acid residues identified at the homo- and heterodimer interfaces are labeled. The black arrow indicates the site of truncation of the N-termini for protein expression in this study.

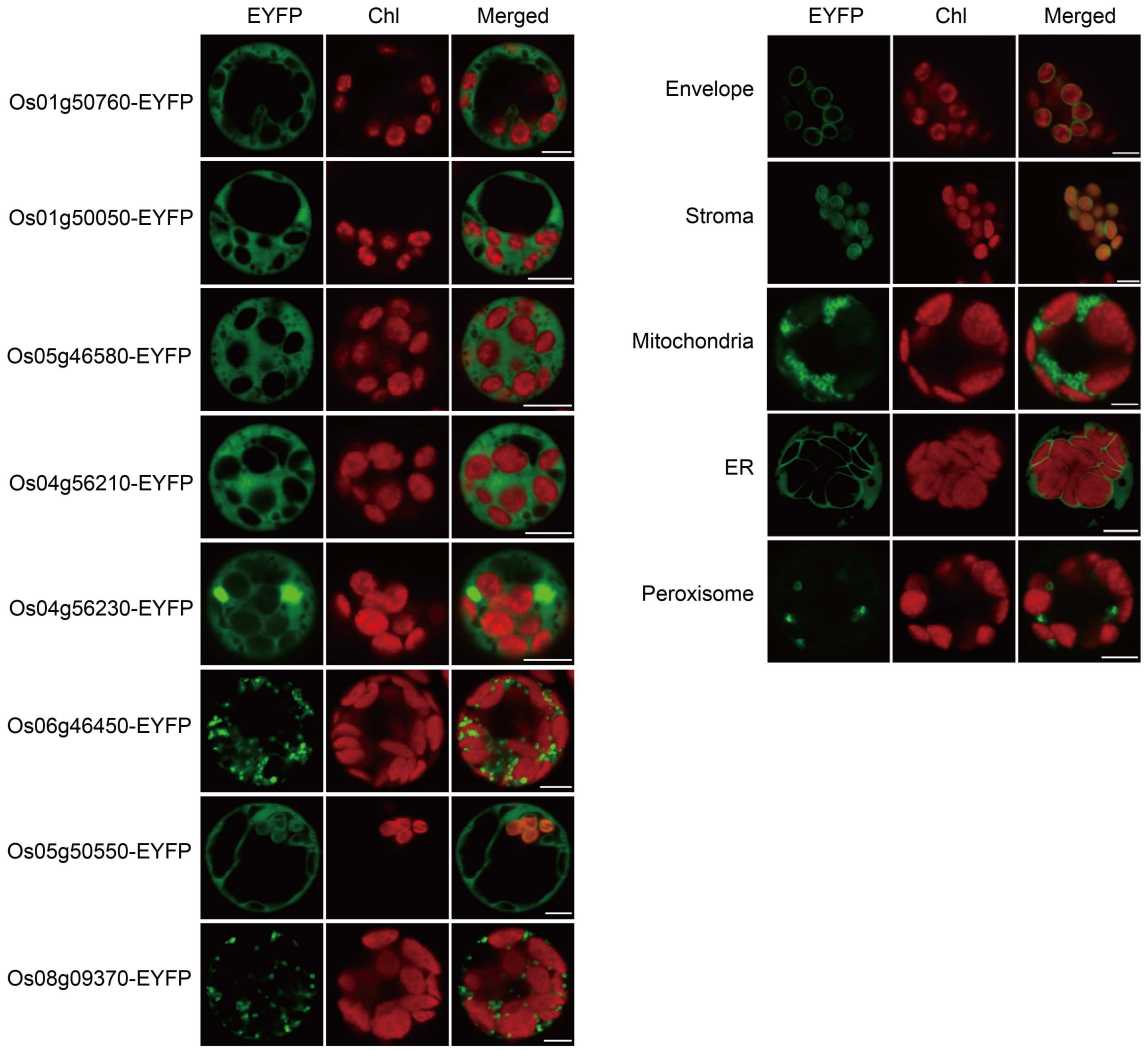

Fig. S2. Subcellular localization of rice PTS homologs. EYFP fusion proteins of rice Tic40 (Os04g35900), Arabidopsis RbcS (At1g67090), rice Rpl6-1 (Os03g51510), Arabidopsis WAK2 (At1g21270) and rice PMP22 (Os02g13270) were used as markers for the localization of the envelope and stroma in chloroplasts, mitochondria, endoplasmic reticulum (ER) and peroxisomes, respectively. Scale bars = 5 μm.

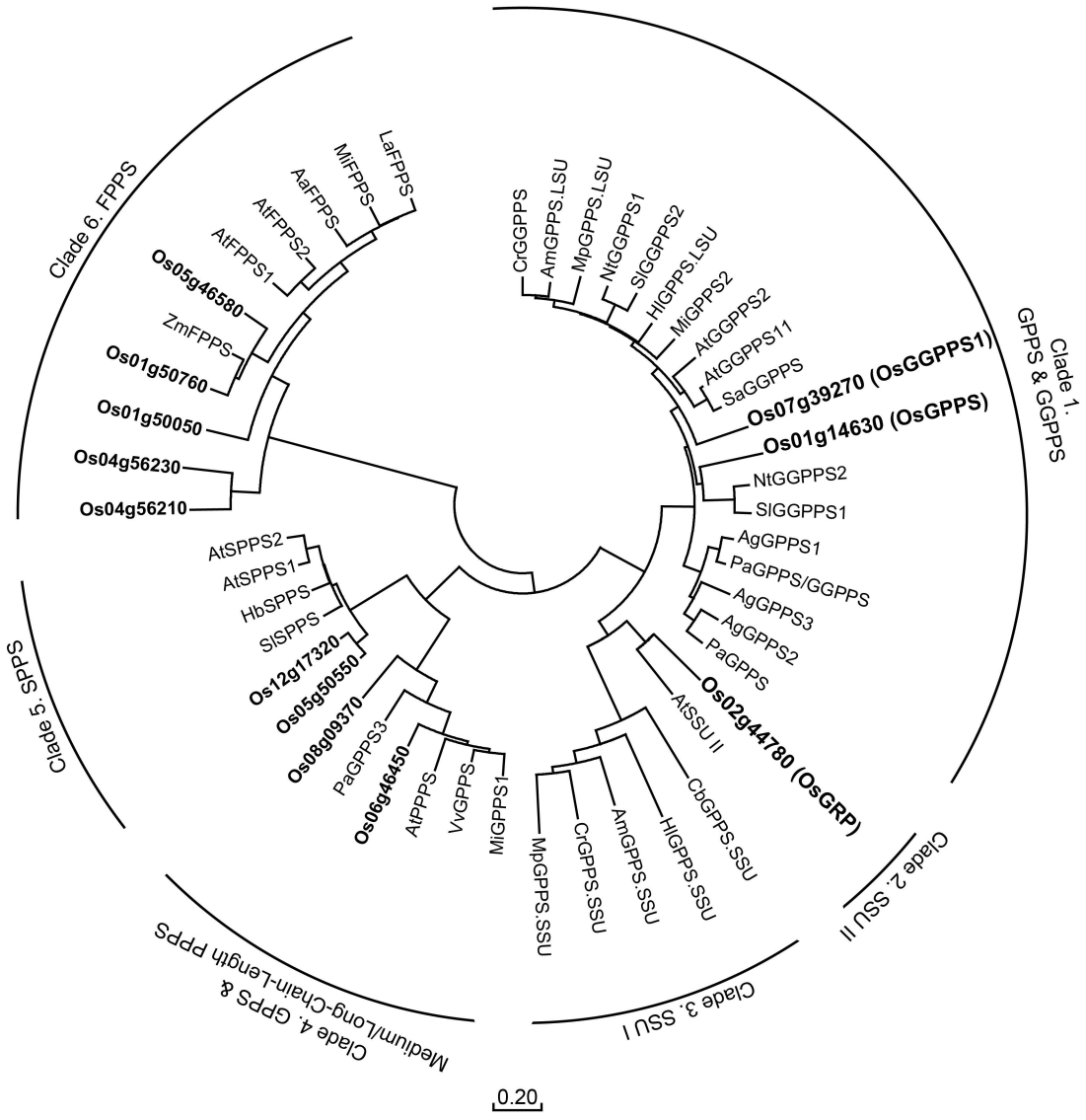

Fig. S3. Phylogenetic analysis of rice PTS homologs and PTSs identified in other plants. The neighbor-joining based phylogenetic tree was constructed using MEGA6 with default settings. The scale bar corresponds to 20% amino acid sequence divergence. The first two letters in each of the homologs are abbreviations for the species (Aa, *Artemisia annua*; Ag, *Abies grandis*; At, *Arabidopsis thaliana*; Am, *Antirrhinum majus*; Cb, *Clarkia breweri*; Cr, *Catharanthus roseus*; Hb, *Hevea brasiliensis*; Hl, *Humulus lupulus*; La, *Lupinus albus*; Mi, *Mangifera indica*; Mp, *Mentha piperita*; Nt, *Nicotiana tabacum*; Os, *Oryza sativa*; Pa, *Picea abies*; Sa, *Sinapis alba*; Sl, *Solanum lycopersicum*; Vv, *Vitis vinifera*; Zm, *Zea mays*). Rice PTS homologs are shown in bold.

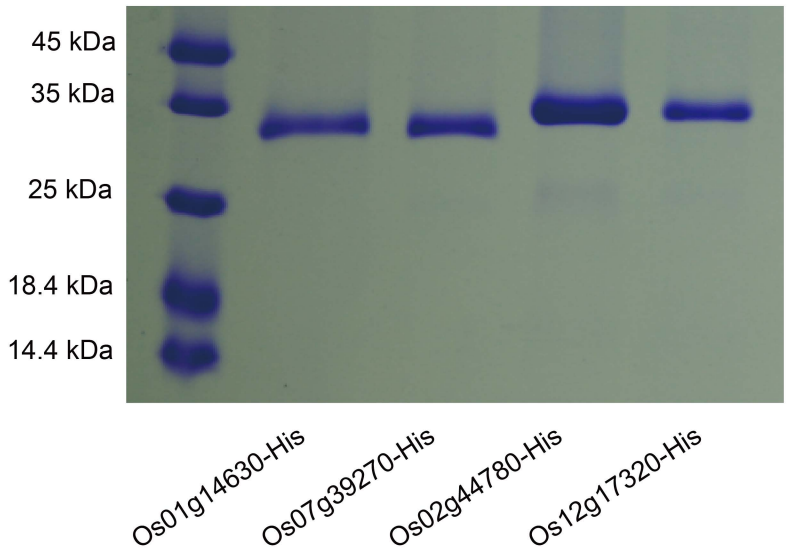

Fig. S4. SDS-PAGE analysis of recombinant rice PTS homologs that have chloroplast localization. Recombinant proteins with His-Tag at their C-termini were heterologously expressed in *E. coli* and purified using Ni-NTA agarose under native conditions.

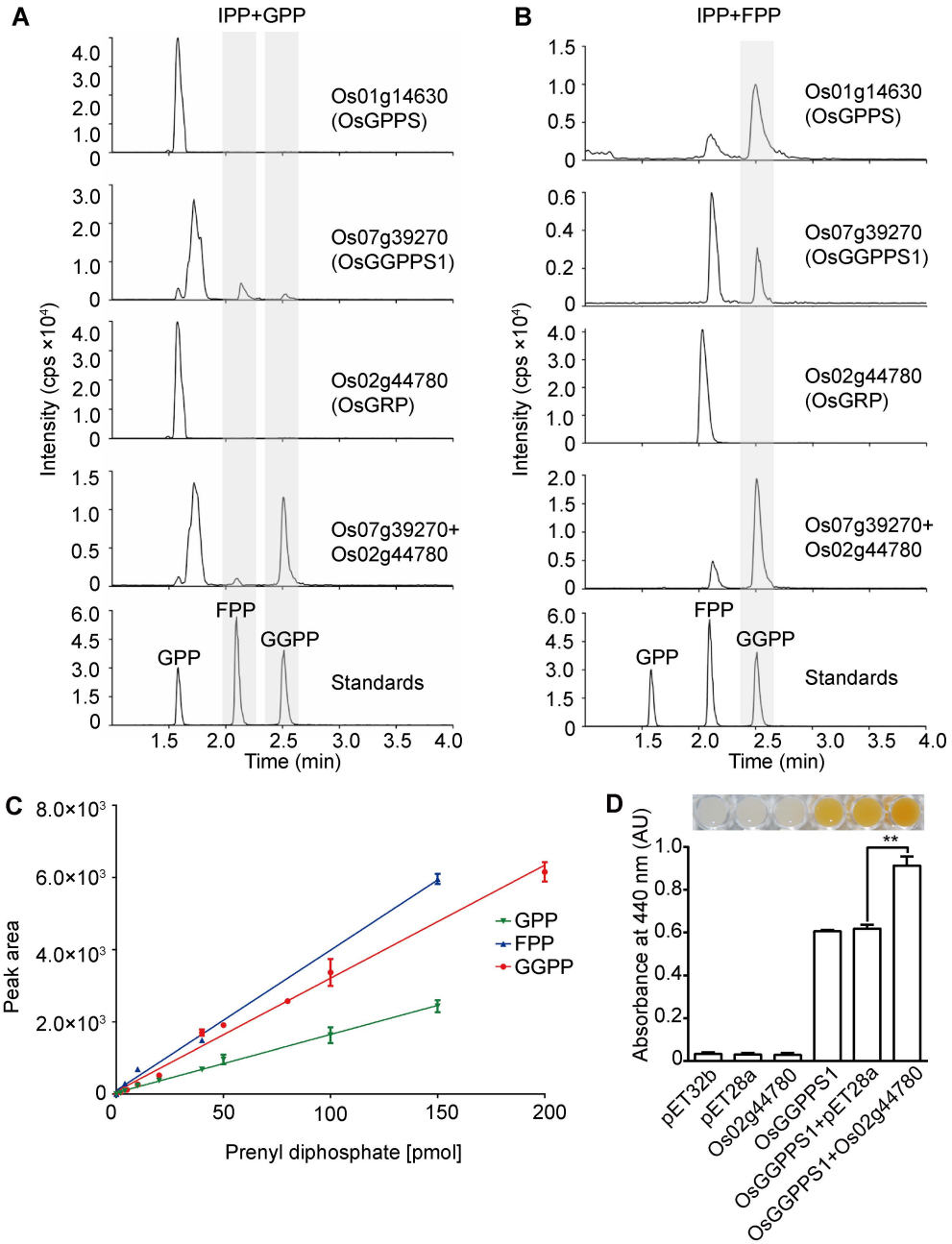

Fig. S5. Enzyme activity assay of rice PTSs. (*A* and *B*) LC-MS/MS chromatograms showing the products generated by Os01g14630 (OsGPPS), Os07g39270 (OsGGPPS1), Os02g44780 (OsGRP), and a mixture of equal amounts of Os07g39270 and Os02g44780 from IPP plus GPP (*A*) and IPP plus FPP (*B*) *in vitro*. Results shown are reprenstatives of three independent experiments. (*C*) Calibration curves for quantification of GPP, FPP and GGPP measured by LC-MS/MS under the conditions decribed. R^2 for linear regression was 0.98 for GPP and GGPP, and was 0.99 for FPP. At least four individual dilution series with two injections each were analyzed under the conditions described. Data are means ± SEM (n = 3). (*D*) Color complementation assay for detecting GGPPS activity of OsGGPPS1 with Os02g44780. BL21(DE3) cells were co-transformed with pAC-94N and expression vectors harboring rice *PTS* genes. For co-expression, *Os02g44780* was cloned in pET28a and *OsGGPPS1* was cloned in pET32b. Both constructs were co-transformed with pAC-94N. Data are means ± SEM (n = 3). $^{**}P < 0.01$; Student's t test.

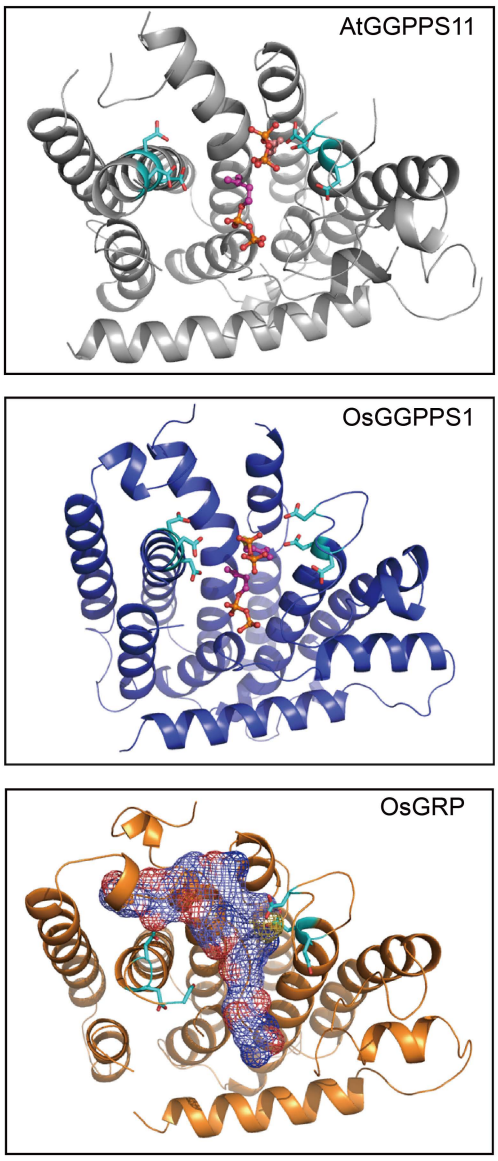

Fig. S6. Overall structures of AtGGPPS11(PDB ID: 5E8L), OsGGPPS1 and OsGRP (top view). The structures are shown as cartoon and colored in grey (AtGGPPS11), blue (OsGGPPS1) and orange (OsGRP). The aspartate-rich motifs are highlighted with cyan sticks. In structures of AtGGPPS11 and OsGGPPS1, substrate DMAPP and IPP (orange sticks) are superimposed in the binding pocket using the PDB model 1UBX and 1RQI. In OsGRP, the loop in the binding pocket is shown with mesh (Blue and Red). Images were produced using PyMol.

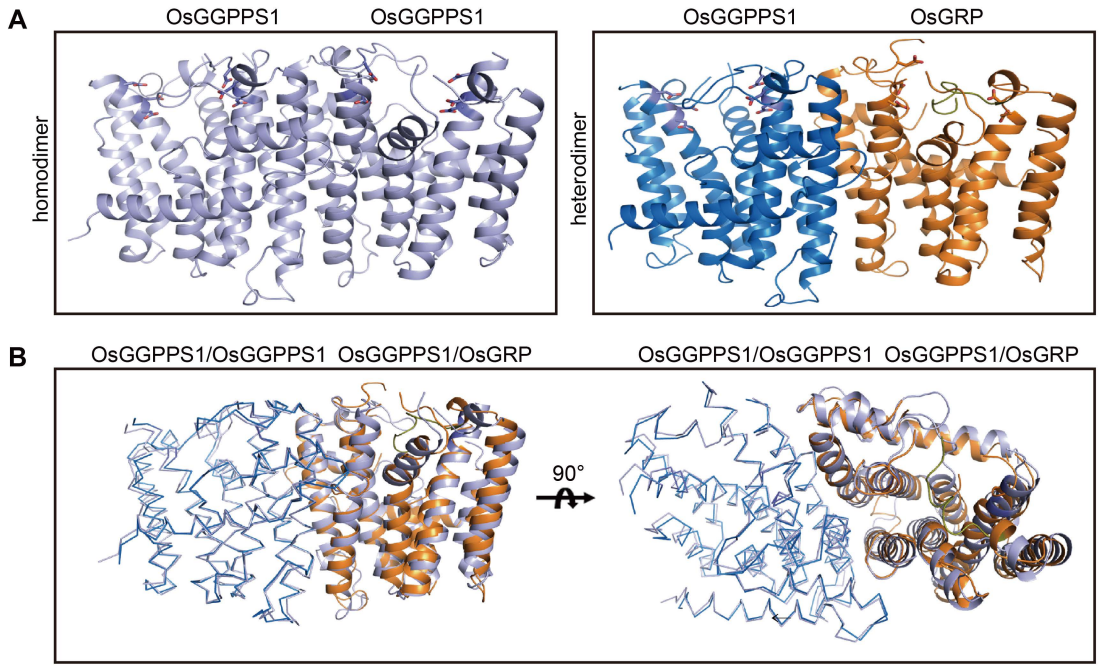

Fig. S7. Structures of OsGGPPS1 homo- and heterodimers. (*A*) Overall structures of homodimeric OsGGPPS1/OsGGPPS1 and heterodimeric OsGGPPS1/OsGRP (side view). (*B*) Superimposed structures of homodimeric and heterodimeric OsGGPPS1 viewed from two orientations. The same OsGGPPS1 subunit in both structures is shown as ribbons, and the other OsGGPPS1 subunit in the homodimer as well as the OsGRP subunit in the heterodimer are shown as cartoon. In (*A*) and (*B*), the structures are colored in light blue (OsGGPPS1 in homodimer), blue (OsGGPPS1 in heterodimer) and gold (OsGRP in heterodimer), respectively. Images were produced using PyMol.

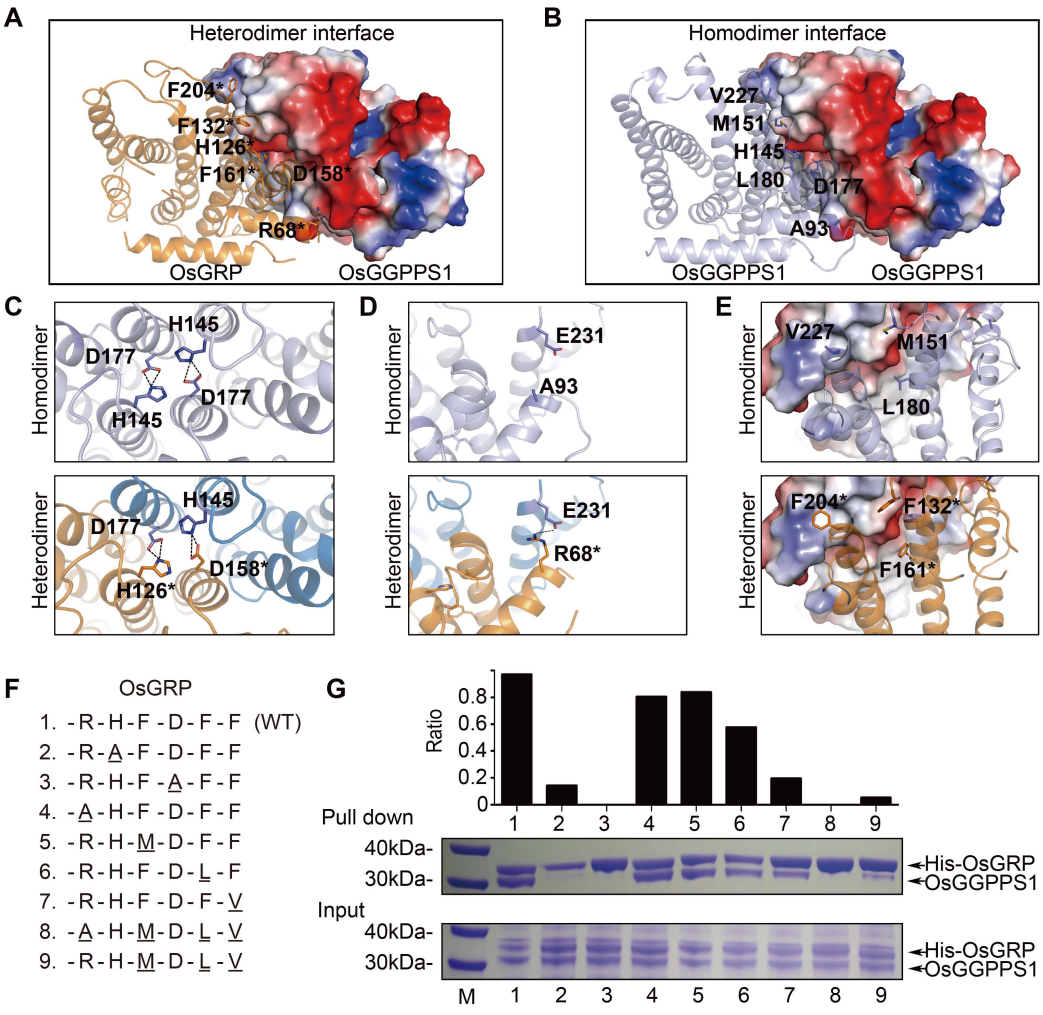

Fig. S8. Effects of interface amino acid residues on OsGGPPS1 - OsGRP interaction. (*A*,*B*) Key residues on the interfaces of OsGGPPS1 homodimer and OsGGPPS1/OsGRP heterodimer. Residues from OsGRP of the heterodimer (indicated by *) (*A*) and from its counterpart OsGGPPS1 of the homodimer (*B*) were labelled. The other OsGGPPS1 proteins in homo- and heterodimers are shown with electrostatic potential surface (blue and red colors represent positive and negative charges, respectively). (*C*,*D* and *E*) Comparison of the key residues on the interfaces. Hydrogen bonds are represented by dark dashed lines. (*F*) Sequence comparisons of wild type (1.) and mutated OsGRP (2.-9.). Mutated amino acids of OsGRP are underlined. (*G*) Pull down analysis of OsGGPPS1 binding to His-tagged WT and mutated OsGRP. Lane numbers correspond to mutants in (*F*). Arrows show the position of His-OsGRP and untagged OsGGPPS1 in the pull down samples separated by SDS-PAGE.

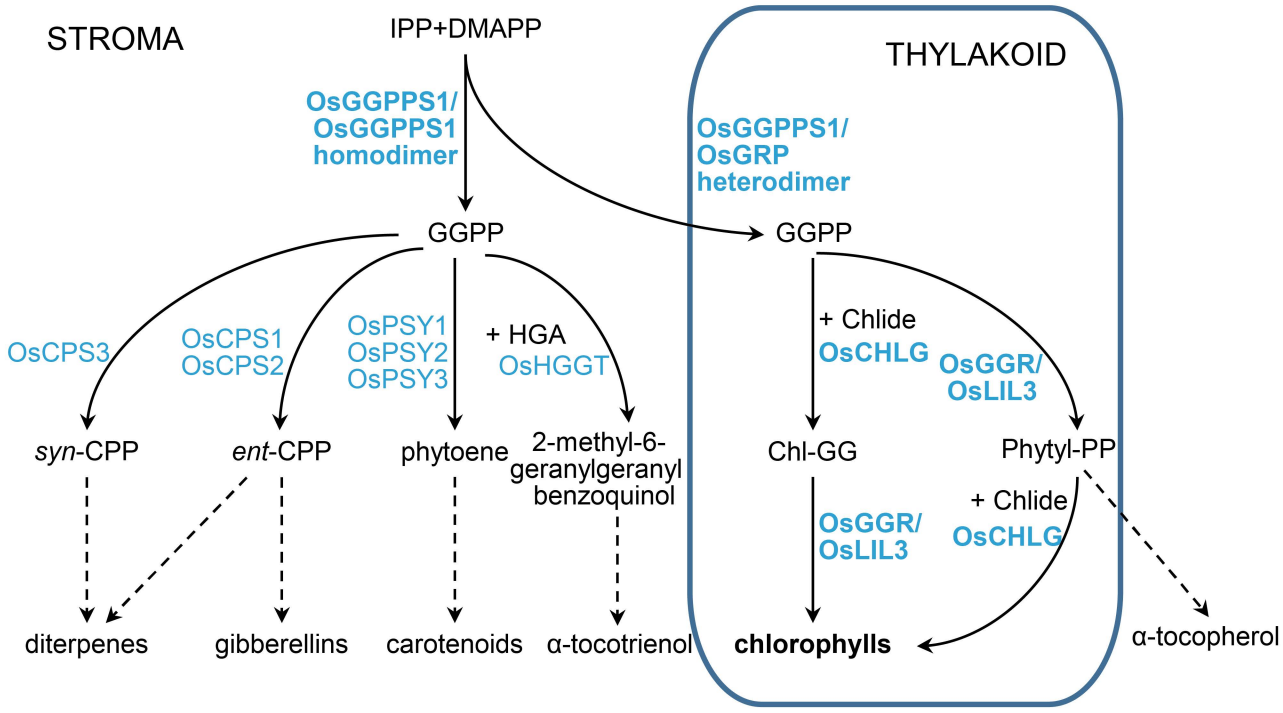

Fig. S9. Schematic overview of the metabolic pathways downstream of GGPP in rice chloroplasts. IPP, isopentenyl diphosphate; DMAPP, dimethylallyl diphosphate; GGPP, geranylgeranyl diphosphate; CPP, copalyl diphosphate; HGA, homogentisate. Enzymes and interacting proteins are shown in blue: GGPPS, geranylgeranyl diphosphate synthase; GRP, GGPPS Recruiting Protein; PSY, phytoene synthase; CPS, CPP synthase; CHLG, chlorophyll synthase; GGR, geranylgeranyl reductase; LIL3, light-harvesting-like protein 3; HGGT, homogentisate geranylgeranyl transferase.

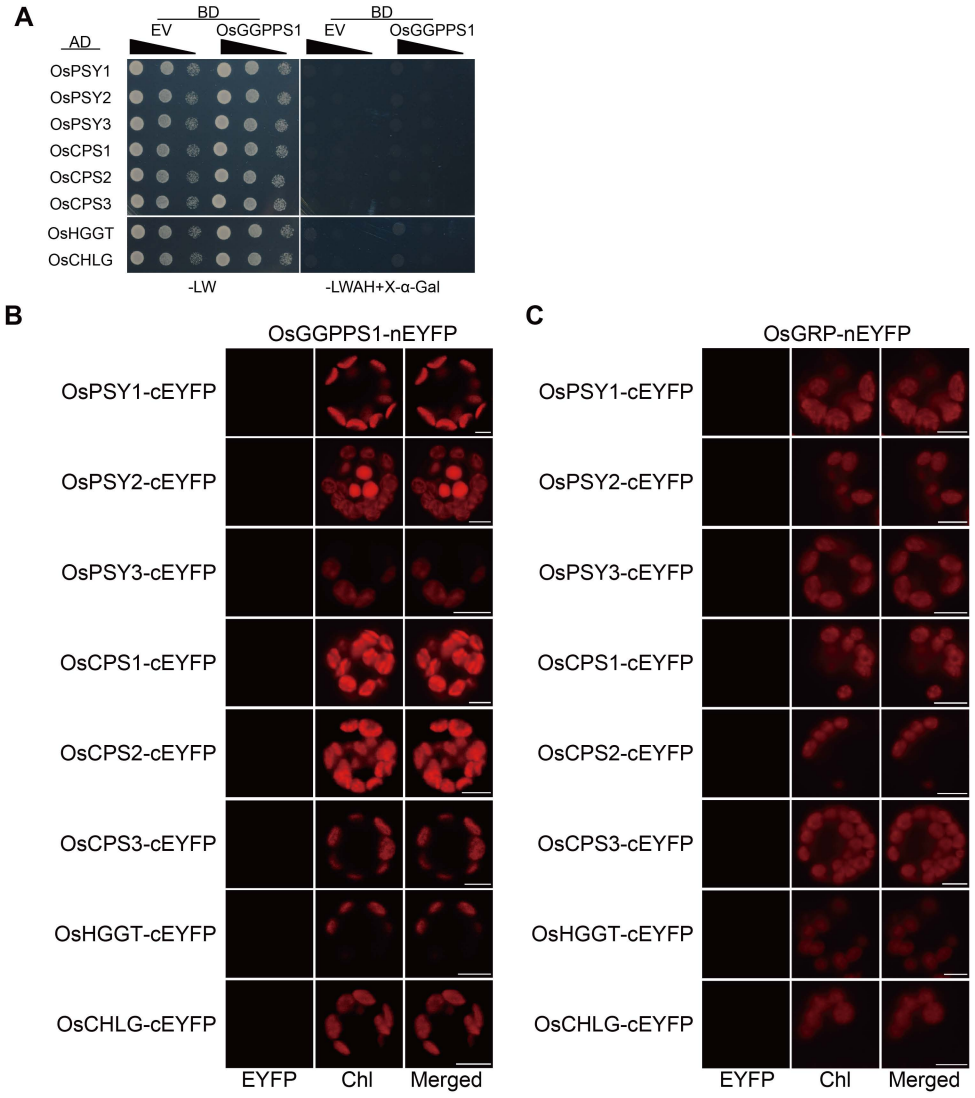

Fig. S10. OsGGPPS1 and OsGRP do not interact with most of the downstream terpenoid biosynthetic enzymes. (*A*) Yeast two-hybrid assay of protein-protein interactions between OsGGPPS1 and candidate partners. OsGGPPS1 was fused with the DNA binding domain (BD) of pGBK-T7 and candidate partners were fused with the activation domain (AD) of pGAD-T7. EV, empty vector. Ten-fold serial dilutions of yeast cells expressing both fusion proteins were spotted on nonselective (-LW) medium and selective medium supplied with X-α-Gal (-LWAH+X-α-Gal). (*B* and *C*) BiFC detection for the interactions of OsGGPPS1 (*B*) and OsGRP (*C*) with downstream terpenoid biosynthetic enzymes in rice leaf protoplasts. Chl, chlorophyll autofluorescence. Scale bars = 5 μm.

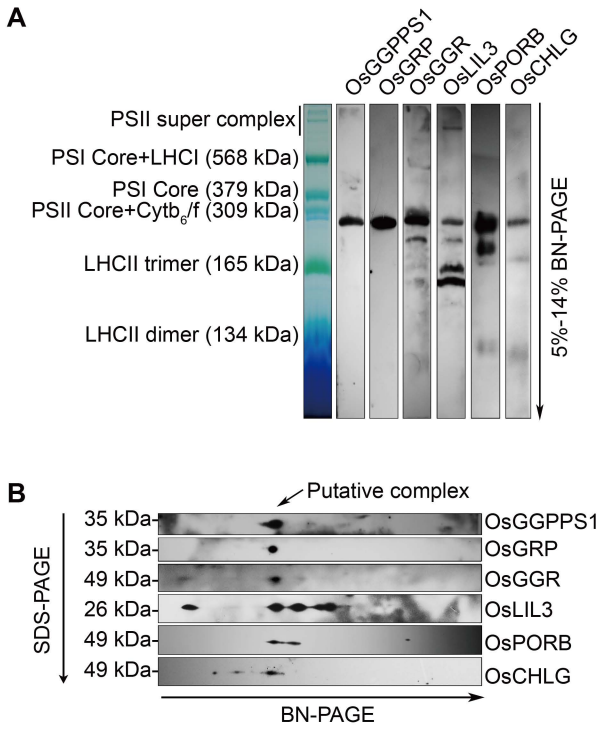

Fig. S11. BN-PAGE analysis of the co-localization of the OsGGPPS1/OsGRP heterodimer with OsGGR, OsLIL3, OsPORB and OsCHLG in thylakoid membranes. (*A*) Rice thylakoid membrane complexes were separated by BN-PAGE and immunoblotted with corresponding antibodies. (*B*) 2D BN/SDS-PAGE and immunoblotting analysis of the protein complex.

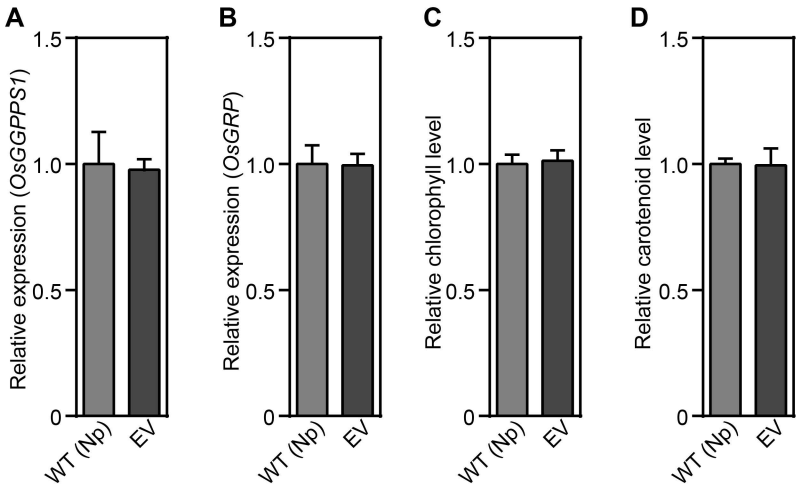

Fig. S12. Quantification of *OsGGPPS1* (*A*) and *OsGRP* (*B*) transcript levels, chlorophyll (*C*) and carotenoid (*D*) levels in wild type and empty vector (EV) control lines. In each study, corresponding WT level was set as 1. Data are means ± SEM (n = 3).

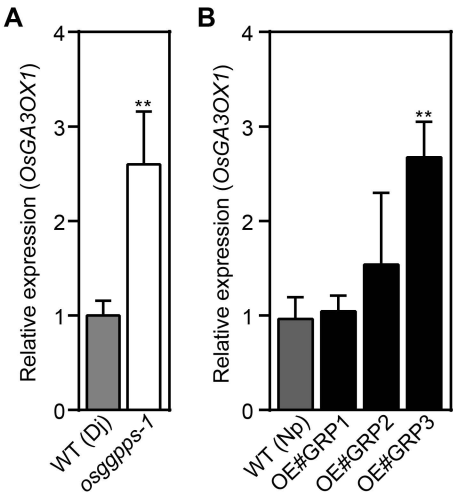

Fig. S13. Quantification of *OsGA3OX1* gene expression in *OsGGPPS1* T-DNA insertion (*A*) and *OsGRP* overexpression lines (*B*). In each study, corresponding WT level was set as 1. Data are means ± SEM ($n = 3$). $^{**}P < 0.01$; Student's *t* test.

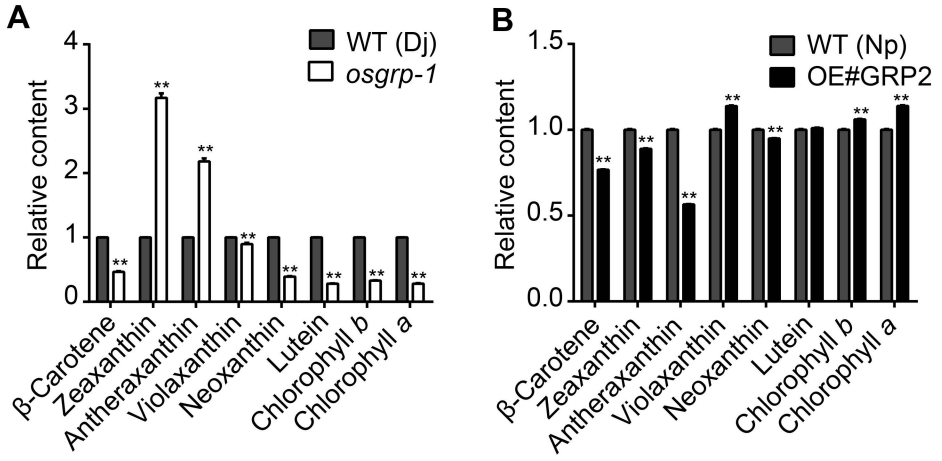

Fig. S14. Carotenoid and chlorophyll contents in the leaves of control and *OsGRP* T-DNA insertion (*A*) and overexpression lines (*B*). In each study, corresponding WT level was set as 1. Data are means ± SEM ($n = 3$). $^{**}P < 0.01$; Student's *t* test.

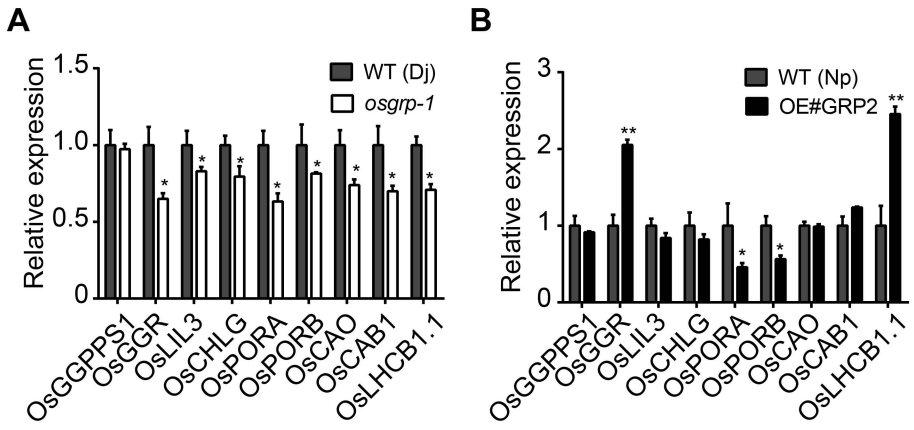

Fig. S15. Quantification of chlorophyll biosynthestic gene transcript levels in *OsGRP* T-DNA insertion (*A*) and overexpression lines (*B*). In each study, corresponding WT level was set as 1. OsGGPPS1, geranylgeranyl diphosphate synthase 1; OsGGR, geranylgeranyl reductase; OsLIL3, light-harvesting-like protein 3; OsCHLG, chlorophyll synthase; OsPORA/B, protochlorophyllide oxidoreductase A/B; OsCAO, chlorophyllide *a* oxygenase; OsCAB1, chlorophyll *a*/*b* binding protein 1; OsLHCB1.1, light harvesting chlorophyll *a*/*b* binding protein 1.1. Data are means ± SEM ($n = 3$). *$P < 0.05$, **$P < 0.01$; Student's *t* test.

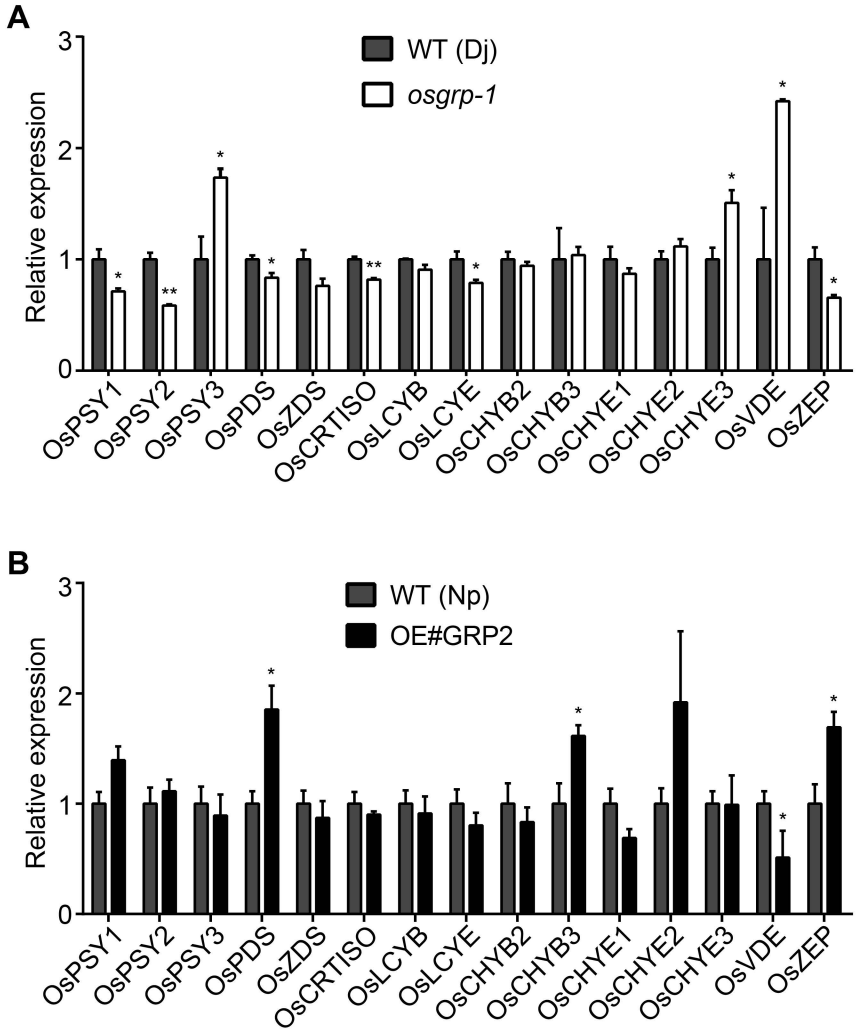

Fig. S16. Quantification of carotenoid biosynthestic gene transcript levels in *OsGRP* T-DNA insertion (*A*) and overexpression lines (*B*). In each study, corresponding WT level was set as 1. OsPSY, phytoene synthase; OsPDS, phytoene desaturase; OsZDS, ζ-carotene desaturase; OsCRTISO, carotenoid isomerase; OsLCYB, lycopene β-cyclase; OsLCYE, lycopene ε-cyclase; OsCHYB, carotene β-hydroxylase; OsCHYE, carotene ε-hydroxylase; OsVDE, violaxanthin de-epoxidase; OsZEP, zeaxanthin epoxidase. Data are means ± SEM ($n = 3$). *$P <$ 0.05, **$P < 0.01$; Student's t test.

Table S1. List of the rice PTS homologs.

Gene ID	Function/Annotation	Protein length (Amino acids)	Conserved aspartate-rich motifs
Os01g14630	polyprenyl synthase, putative	376	DDMPCMD / DDVLD
Os01g50050	polyprenyl synthase, putative	356	DDIMD / DDYLD
Os01g50760	farnesyl diphosphate synthase 1	353	DDIMD / DDYLD
Os02g44780	polyprenyl synthase, putative	342	DDLPCFD / DDIRS
Os04g56210	polyprenyl synthase, putative	392	DDIMD / DDYLD
Os04g56230	polyprenyl synthase, putative	407	DDITD / DDYLD
Os05g46580	polyprenyl synthase, putative	355	DDIMD / DDYLD
Os05g50550	solanesyl diphosphate synthase 2	403	DDVID / DDILD
Os06g46450	solanesyl diphosphate synthase 1	426	DDVLD / DDVLD
Os07g39270	polyprenyl synthase, putative	366	DDLPCMD / DDILD
Os08g09370	polyprenyl synthase, putative	412	DDVLD / DDILD
Os12g17320	polyprenyl synthase, putative	414	DDVID / DDILD

Table S2. Kinetic parameters for homodimeric and heterodimeric OsGGPPS determined using LC/MS-MS analysis.

	K_m for DMAPP, μM	V_{max}, nmol/min/mg
OsGGPPS1	9.56 ± 0.91	2.69 ± 0.07
OsGGPPS1/Os02g44780 (OsGRP) (1:1)	12.14 ± 2.11	11.59 ± 0.53
OsGGPPS1/Os02g44780 (OsGRP) (1:2)	12.26 ± 3.23	11.66 ± 0.68

Data are means ± SD (n =3 independent experiments).

Table S3. Statistics for data collection and structure refinement.

	OsGGPPS1/OsGRP	OsGGPPS1/OsGGPPS1
Data collection statistics		
Space group	P1	$P2_1$
Cell dimensions		
a, *b*, *c* (Å)	103.0, 102.9, 103.4	56.0, 74.1, 71.3
α, *β*, *γ* (º)	109.3, 109.6, 109.1	90, 90.8, 90
Wavelength (Å)	0.9793	0.9793
Resolution range (Å)[a]	37.7−3.6 (3.72−3.6)	38.1−2.0 (2.07−2.0)
R_{merge}(%)[a]	0.122 (0.679)	0.082 (0.517)
$I/\sigma I$[a]	8.26 (1.53)	19 (2.4)
Completeness (%)[a]	96.9 (91.2)	99.2 (94.3)
Redundancy	1.9	4
Refinement		
Resolution range (Å)	37.3−3.6	38.1−2.0
No. of reflections	36,920	39,062
R_{work}/R_{free}[b]	0.251/0.263	0.187/0.213
No. of atoms	12,390	4,538
Protein	12,390	4.312
Water	0	226
Average *B* factors (Å^2)	91.4	33.1
Protein	91.4	32.5
Solvent		43.5
R.m.s deviations		
Bond lengths (Å)	0.013	0.011
Bond angles (º)	2.51	1.37
Ramachandran plot		
Favored (%)	89	98
Allowed (%)	11	2

[a] Values in parentheses represent the highest-resolution shells.

[b] $R = \Sigma_{hkl} ||F_o|-|F_c|| / \Sigma_{hkl}|F_o|$

Table S4. Primers used in this work.

Prime Name[1]	Sequence (5'-3')[2]
For protein expression	
In pET32b	
δOsGPPS-NdeIF	GCTAATCCATATGGGTAGCTTCGACTTTCAGCGG
OsGPPS-EcoRIR	GGAATTCCAATGCTGCCTGTAGGCGATGAAC
δOsGGPPS1-NdeIF	GCTAATCCATATGACGGGGTTTGATTTTAACGCG
OsGGPPS1-EcoRIR+	GGAATTCTCAGTTCTGCCGATAGGCAATATAATTG
OsGGPPS1-XhoIR	CAGCTCGAGGTTCTGCCGATAGGCAATATAATTGG
δOsGRP-NdeIF	GCTAATCCATATGTCCTTCGATTTGCGCCTCTATTG
OsGRP-EcoRIR	GGAATTCCACGGCGTTGTAGCTGCATC
δOs12g17320-NdeIF	GGAATTCCATATGGGTGTTTGCTCCGTGGTCT
Os12g17320-XhoIR	CCGCTCGAGATCAATCCTTTCTAGATTATATTTCAC
δAmLSU-NdeIF	GCTAATCCATATGAACCCACAAGAATCAAGCCAAAAAAC
AmLSU-EcoRIR	GGAATTCCAATTATCTCTATAAGCGATGTAGTTAGC
In pET28a	
δOsGRP-EcoRIF	CGGAATTCTCCTTCGATTTGCGCCTCTATTG
OsGRP-HindIIIR+	CCCAAGCTTCTACGGCGTTGTAGCTGCATC
For site-directed mutagenesis[3]	
OsGRP-R68A-F	CGCGATGCCCATCCGCACGCCGGAGgctATCCACTCCGCC
OsGRP-R68A-R	CGGCGTAGCGCATGGCGGAGTGGATagcCTCCGGCGTGCGG
OsGRP-H126A-F	GATGCTCCACGCGGCGTCGCTCGTGgctGACGACCTCCCA
OsGRP-H126A-R	CGGCGTCGAAGCATGGGAGGTCGTCagcCACGAGCGACGC
OsGRP-D158A-F	CACCGACATGGCCGTCCTCGCCGGGgctGCGCTCTTCCCC
OsGRP-D158A-R	GGGTGTAGGCGAGGGGGAAGAGCGCagcCCCGGCGAGGAC
OsGRP-F132M-F	GCTCGTGCACGACGACCTCCCATGCatgGACGCCGCGCCC
OsGRP-F132M-R	GCCCGCGGCGGGTGGGCGCGGCGTCcatGCATGGGAGGTC
OsGRP-F161L-F	GGCCGTCCTCGCCGGGGACGCGCTCctcCCCCTCGCCTAC
OsGRP-F161L-R	CGATGACGTGGGTGTAGGCGAGGGGgagGAGCGCGTCCCC
OsGRP-F204V-F	ATCCACAGGCATGGCGGCCGGCCAAgtcCTCGACCTCGCC
OsGRP-F204V-R	GGGCGGTGGCGCCGGCGAGGTCGAGgacTTGGCCGGCCGC
For constructing plant transformation vectors	
In pRTL2	
OsGGPPS1-KpnIF	GGGGTACCATGGCTGCCTTCCCCCCG
OsGGPPS1-BamHIR	CGGGATCCTCAGTTCTGCCGATAGGCAATATAATTGG

OsGRP-NcoIF	CATGCCATGGCTCTCTCCTCCTTCTCC
OsGRP-NcoIR	CATGCCATGGCTACGGCGTTGTAGCTGCATC
In pFGC5941	
OsGRP-AscIF-i	TTGGCGCGCCGTCATCGCCCACACTCCGTC
OsGRP-SwaIR-i	CCATTTAAATCTACGGCGTTGTAGCTGCATCC
OsGRP-XbaIF-i	GCTCTAGACTACGGCGTTGTAGCTGCATCC
OsGRP-SmaIR-i	TCCCCCGGGGTCATCGCCCACACTCCGTC
OsGGPPS1-BamHIF-i	CGGGATCCGTACCGCATCGCCTCGTGGA
OsGGPPS1-SmaIR-i	TCCCCCGGGGTCGCAACTCACGGTCGCAGT
OsGGPPS1-AscIF-i	TTGGCGCGCCGTCGCAACTCACGGTCGCAGT
OsGGPPS1-SwaIR-i	CCATTTAAATGTACCGCATCGCCTCGTGGA

For subcellular localization and BiFC assays

In pA7-EYFP	
OsGPPS-SpeIF	GGACTAGTATGCACGTCCTCGCTCAATC
OsGPPS-SpeIR	GGACTAGTATGCTGCCTGTAGGCGATG
OsGGPPS1-FL-SpeIF	GGACTAGTATGGCTGCCTTCCCCCCG
OsGGPPS1-FL-SpeIR	GGACTAGTGTTCTGCCGATAGGCAATATAATTGG
OsGGPPS1-cTP-SpeIR	GGACTAGTCGCAGCCTTCTCACCCATATACGC
OsGRP-SpeIF	GGACTAGTATGGCTCTCTCCTCCTTCTC
OsGRP-SpeIR	GGACTAGTCGGCGTTGTAGCTGCATCC
Envelope (Tic40)-SpeIF	GGACTAGTATGGAGAGCCTGGTCCTCG
Envelope (Tic40)-SpeIR	GGACTAGTGCCATTAATTTGAGGGAAGATTTGTG
Stroma (RbTP)-SpeIF	GGACTAGTATGGCTTCCTCTATGCTCTC
Stroma (RbTP)- SpeIR	GGACTAGTCCACACCTGCATGCAGTTAAC
Mito (OsRpl6-1)-SpeIF	GGACTAGTATGGAGGCCAAGGTTTTC
Mito (OsRpl6-1)-SpeIR	GGACTAGTGGGTTTGAAGCAGAAGAC
ER (AtWAK2)-SpeIF	GGACTAGTATGAAGGTACAGGAGGGTTTGTTC
ER (AtWAK2)-SpeIR	GGACTAGTAGTTTGGCACTCCTTGCGAGG
Pero (OsPMP22)-SpeIF	GGACTAGTATGGCAGCAGCAGCAGTAGCAGCAG
Pero (OsPMP22)-SpeIR	GGACTAGTCGACTGCTTCAAAGACATGGCCCTTG
OsFPPS1-SpeIF	GGACTAGTATGGCGGCGGCGGTGGTG
OsFPPS1-SpeIR	GGACTAGTCTTCTGCCTCTTGTAGATCTTGTGC
Os05g46580-SpeIF	GGACTAGTATGGCGGCGGCGAATGGGAG
Os05g46580-SpeIR	GGACTAGTCTTCTGTCTCTTGTAGATCTTGTGC
Os01g50050-SpeIF	GGACTAGTATGGCCGCCGCGGGTGCG
Os01g50050-SpeIR	GGACTAGTCTTGCTCCTCTTGTAGATCTTGTGC
Os04g56210-SpeIF	GGACTAGTATGTCCATGCAGGAGATGCTC

Os04g56210-SpeIR	GGACTAGTCTTCTTCCTTTGATGAATTTTCTTCAG
Os04g56230-SpeIF	GGACTAGTATGGGGGCGCTGGCGGCG
Os04g56230-SpeIR	GGACTAGTCTTCTTCCTCCTGTAAATCTTCTTCAG
OsSPPS1-SpeIF	GGACTAGTATGTCGTGGCGGTGGGCTC
OsSPPS1-SpeIR	GGACTAGTTTTTGTTCTAGTGATGACTCTCTCTGTGAT GTC
OsSPPS2-SpeIF	GGACTAGTATGTTGTCTGTGAGCTGCCCG
OsSPPS2-SpeIR	GGACTAGTGTCAATCCTCTGAAGATTATATTTCACC
Os08g09370-SpeIF	GGACTAGTATGCTACTGCCGAGGCGTCTTC
Os08g09370-SpeIR	GGACTAGTCTTTGTTCTCTTGATGAGCTTTTCTGTAAG
Os12g17320-BamHIF	CGGGATCCATGGCGGCGCCGTCCTCC
Os12g17320-BamHIR	CGGGATCCATCAATCCTTTCTAGATTATATTTC

In pSAT1A-cEYFP-N1, pSAT4A-nEYFP-N1 and pSAT4A-mCherry-N

OsGGPPS1-XhoIF	CCGCTCGAGATGGCTGCCTTCCCCCCG
OsGGPPS1-EcoRIR	CGGAATTCGTTCTGCCGATAGGCAATATAATTGGC
OsGRP-BglIIF	GAAGATCTATGGCTCTCTCCTCCTTCTCCATG
OsGRP-EcoRIR	CGGAATTCCGGCGTTGTAGCTGCATCCTG
OsGGR-XhoIF	CCGCTCGAGATGACCTCGCTGTCGTCCTC
OsGGR-EcoRIR	CGGAATTCCAAGGTGACCTTCTCCATCTC
OsLIL3-EcoRIF	CGGAATTCATGGCCATGGCGACCTCCAC
OsLIL3-BamHIR	CGGGATCCATTTCTTGGGCTGAGAAGGGGACTC
OsCPS1-XhoIF	CCGCTCGAGATGATTCACCTCCACTCCCCGC
OsCPS1-EcoRIR	CGGAATTCGGTGTTGATGACGCGGTCGTAG
OsCPS2-XhoIF	CCGCTCGAGATGCAGATGCAGGTGCTCACC
OsCPS2-EcoRIR	CGGAATTCCCTCCAGAGGTTGTCCTGGATGTAG
OsCPS3-XhoIF	CCGCTCGAGATGCCGGTCTTCACTGCATCATTC
OsCPS3-EcoRIR	CGGAATTCCCAGTCTTCTTCCTCATGGGCCAAC
OsPSY1-XhoIF	CCGCTCGAGATGGCGTCCTCCTCGTCGG
OsPSY1-EcoRIR	CGGAATTCTGATGCAACTGCCGCTCTTG
OsPSY2-EcoRIF	CGGAATTCATGATGTCCACCACCACCACC
OsPSY2-BamHIR	CGGGATCCATGATGATGTTAGGCTAGAGCAGTGC
OsPSY3-XhoIF	CCGCTCGAGATGGCGGCCATCACGCTC
OsPSY3-EcoRIR	CGGAATTCCTTCTGGCTATTTCTCAGTGAGTAGG
OsCHLG-XhoIF	CCGCTCGAGATGGCCACCTCCCACCTCC
OsCHLG-EcoRIR	CGGAATTCGTGGCTGGTTGCAAGGGCG
OsHGGT-XhoIF	CCGCTCGAGATGCAAGCCTCATCGGCGG
OsHGGT-BamHIR	CGGGATCCGCTGCACAAATGGTATAAGGAAATACTC
Stroma (RbTP)-XhoIF	CCGCTCGAGATGGCTTCCTCTATGCTCTC

Stroma (RbTP)-EcoRIR	CGGAATTCCCACACCTGCATGCAGTTAAC
For Y2H assay vectors	
In pGAD-T7	
AtGGPPS11-EcoRIF	CGGAATTCATGGCTTCAGTGACTCTAGG
AtGGPPS11-BamHIR	CGGGATCCTCAGTTCTGTCTATAGGCAATGTAATTAG
OsPSY1-EcoRIF	CGGAATTCATGGCGTCCTCCTCGTCGG
OsPSY1-XhoIR	CCGCTCGAGTCATGATGCAACTGCCGCTCTTG
OsPSY2-EcoRIF	CGGAATTCATGATGTCCACCACCACCACC
OsPSY2-BamHIR	CGGGATCCTCATGATGATGTTAGGCTAGAGCAGTG
OsPSY3-EcoRIF	CGGAATTCATGGCGGCCATCACGCTC
OsPSY3-XhoIR	CCGCTCGAGCTACTTCTGGCTATTTCTCAGTGAGTAGG
OsCPS1-EcoRIF	CGGAATTCATGATTCACCTCCACTCCC
OsCPS1-ClaIR	CCATCGATTCAAATAACTTGCTCAAAAATCACTTCAG
OsCPS2-EcoRIF	CGGAATTCATGCAGATGCAGGTGCTCACC
OsCPS2-BamHIR	CGGGATCCCTAATTGACATCCTCGAACAAAACC
OsCPS3-EcoRIF	CGGAATTCATGCCGGTCTTCACTGCATCATTC
OsCPS3- BamHIR	CGGGATCCCTAAATCACATCTTGGAATATGACC
OsHGGT-BamHIF	CGGGATCCATGCAAGCCTCATCGGCGG
OsHGGT-XhoIR	CCGCTCGAGTCACTGCACAAATGGTATAAGGAAATAC
OsCHLG-EcoRIF	CGGAATTCATGGCCACCTCCCACCTCC
OsCHLG-XhoIR	CCGCTCGAGTCAGTGGCTGGTTGCAAG
OsGGR-NdeIF	GCTAATCCATATGACCTCGCTGTCGTCCTC
OsGGR-EcoRIR	CGGAATTCTCACAAGGTGACCTTCTCCATCTC
In pGBK-T7	
OsGRP-NcoIF	CATGCCATGGCTCTCTCCTCCTTCTCC
OsGRP-EcoRIR	CGGAATTCCTACGGCGTTGTAGCTGCATC
AtSSU-EcoRIF	CGGAATTCATGTTGTTTAGTGGTTCAGCG
AtSSU-BamHIR	CGGGATCCTCAGAGGGGAAGAAGAAAATGTC
In pGAD-T7 and pGBK-T7	
OsGGPPS1-EcoRIF	CGGAATTCATGGCTGCCTTCCCCCCG
OsGGPPS1-BamHIR	CGGGATCCTCAGTTCTGCCGATAGGCAATATAATTGGCCAGG
For qRT-PCR	
OsGGPPS1-QF	AGGTTGTTGATCTTGAGATGACTG
OsGGPPS1-QR	TCACATCAAGTATATCATCAACAACCTG
OsGRP-QF	GCATCGTAGAGGAGCTCAAA
OsGRP-QR	GCATAGTCCACGAAGCTGTA

OsGGR-QF	GATGATTTCGCCGTCCAACG
OsGGR-QR	GCGCCTCATACCTCAGGAAG
OsLIL3-QF	CGTGCTGCCATGATTGGCTTCTTCATG
OsLIL3-QR	GTCGTCTCATCGATGAGCTTCTTCACTG
OsCHLG-QF	CTGACTTCTTTGTATAGCATAGCTGG
OsCHLG-QR	CTGCAACGGATAATTGAGTTATGTCA
OsPORA-QF	CGGCCTCGTCTGAGTTTATTAT
OsPORA-QR	CCTCTCTCACTGAAAGCTGAAA
OsPORB-QF	GTGAGTGAGAGTGATGTGCTATT
OsPORB-QR	CTCCTCCATCGATCTTTCTTGG
OsCAO-QF	GGGAGACCTGGATGTGTTATG
OsCAO-QR	ATGGTAAGGGCATTGGATTCT
OsCAB1-QF	CCGTAGCTTAGCAGTGGTTAAT
OsCAB1-QR	TCATCATCTCGTCGCACTAAAC
OsLHCB1.1-QF	GGCAAGTGAGTGTGGATCTC
OsLHCB1.1-QR	CAATCTGAACGAACGAAGCAAATA
OsPSY1-QF	CAAATATACTCCGTGACGTTGGAG
OsPSY1-QR	CTACTTCTGGCTATTTCTCAGTGAG
OsPSY2-QF	TTCTACCTAGGTACTCAGCTTATGAC
OsPSY2-QR	CATCACCGGTACTGTCATGAG
OsPSY3-QF	CAAGACATTCTACCTCGCGAC
OsPSY3-QR	CGACGTAGTAGCAGTAGAGGTA
OsPDS-QF	TGCCTATTTTGGTCTTATCATATTTCTGT
OsPDS-QR	TCTTTTTCTCCAGCATGGCATA
OsZDS-QF	GCTGCCCTTTTTGCCTTGA
OsZDS-QR	CACAATAACGAAGAACACACCATTG
OsCRTISO-QF	GGATCTTGCTTCTGCCTGGTA
OsCRTISO-QR	GCTTCAGCTTTTCAGGGATCA
OsLCYB-QF	GGTGCCTCGTCCAGTACGA
OsLCYB-QR	CCATGAACAGCATCTTGTCGAT
OsLCYE-QF	TGCATGAATTTGGCAAATGG
OsLCYE-QR	CCAGCACACGCATCACGTAT
OsCHYB2-QF	TGGCCTGTGGCATGCAT
OsCHYB2-QR	AAGAATAACCATCCCACAGAACATC
OsCHYB3-QF	GCACATGCCATGAGAGCTACTACTA
OsCHYB3-QR	CATAAAATCAGGAAAAGCCAAAACA
OsCHYE1-QF	CATCTGTGCGTGCCTCTTTG
OsCHYE1-QR	AAGTAACAACTCAGCACAATTTCCA

OsCHYE2-QF	GCCGCTGGAAAACAGATAGC
OsCHYE2-QR	CACAGCATCGAAGCATCCAA
OsCHYE3-QF	CCGTTTCAAGCCCAAATTTTAC
OsCHYE3-QR	CCACTGAAAGAGGAAAATGATAGTATGT
OsVDE-QF	ACAACTGTTCCAAATATGATATGGATTATG
OsVDE-QR	TGCCATAAAGTACCGAAGAAAATTAAC
OsZEP-QF	GCACTAAAATGCAGGTTCCACTT
OsZEP-QR	ATGGAGAACTGCAATTTCAATCC
OsGA3OX1-QF	CGATCTCTTCCATGTGCTCACCAAC
OsGA3OX1-QR	CAACGCCGATATATTTGTCCCGAACAAC
OsActin-QF	CATGCTATCCCTCGTCTCG
OsActin-QR	CGCACTTCATGATGGAGTTGT

[1] +, has a stop codon in the sequence. δ, for truncating the N-terminal signal peptide.
[2]Restriction sites are underlined.
[3]Nucleotides in lower case are designed for introducing site-directed mutagenesis.

Table S5. Sequences of peptides synthesized for raising polyclonal antisera in this study.

Protein	Peptide sequence
OsGGPPS1	CLSDAREQLSGFDQE
OsGRP	ELKAQAKMEADRFGC
OsGGR	CAHPIPEHPRPKRVA
OsLIL3	PVETVEAPPSKPEAC
OsPORB	CLSEEASDPEKAKKV
OsCHLG	CNEPYRPIPSGAISE